TÜBİTAK

Turkish Journal of Earth Sciences

http://journals.tubitak.gov.tr/earth/

Research Article

Turkish J Earth Sci
(2015) 24: 209-229

doi:10.3906/yer-1501-14

Clay mineralogy, chemistry, and diagenesis of Late Devonian K-bentonite occurrences in northwestern Turkey

Asuman GÜNAL-TÜRKMENOĞLU[1], Ömer BOZKAYA[2,*], M. Cemal GÖNCÜOĞLU[1], Özge ÜNLÜCE[1], İsmail Ömer YILMAZ[1], Cengiz OKUYUCU[3]

[1]Department of Geological Engineering, Middle East Technical University, Ankara, Turkey
[2]Department of Geological Engineering, Pamukkale University, Denizli, Turkey
[3]Department of Geological Engineering, Selçuk University, Konya, Turkey

Received: 13.01.2015 • **Accepted/Published Online:** 04.03.2015 • **Printed:** 29.05.2015

Abstract: Thin beds of tephra (K-bentonites) formed by the diagenesis of volcanic ash are exposed within the limestone-dolomitic limestone successions of the Yılanlı formation at Zonguldak and Bartın in northwestern Turkey. They were deposited on the Middle Devonian-Lower Carboniferous shallow carbonate platform of the Zonguldak terrane. In this study, K-bentonite samples collected from Gavurpınarı and Yılanlı Burnu limestone quarries are investigated in order to reveal their mineralogical and geochemical characteristics and diagenetic evolution. Illite is the major clay mineral in the studied K-bentonites. Additionally, kaolinite and mixed-layer illite-smectite are identified in some samples. The nonclay minerals calcite, dolomite, quartz, gypsum, feldspar, pyrite, and zircon are also found. Crystal-chemical characteristics (Kübler index, d_{060} values, and polytypes of illites) from two different sampling locations do not show significant variations. Kübler index values for the Yılanlı Burnu and Gavurpınarı sampling locations, 0.47–0.93 (average: 0.71 Δ°2θ) and 0.69–0.77 (average: 0.72 Δ°2θ), respectively, indicate that illites were affected by high-grade diagenetic conditions. The swelling (or smectite) component (~5%), crystallite size (N = 10–20 nm), and polytype ($2M_1 > 1M_d$) data of illites support the same conditions. Illite d_{060} values of 1.491–1.503 Å correspond to a range of octahedral Mg+Fe values of 0.27–0.51 atoms per formula, indicating a composition between end-member muscovite and phengite unit. Trace and rare earth element-based chemical classification of the K-bentonite samples revealed that composition of original volcanic ash is basaltic. Illitization took place by fixation of K from volcanic minerals and ash, and diffusion of elements (Mg+Fe) into and out of the beds during diagenesis. Mineralogical-chemical data point out that these K-bentonites evolved in high-grade diagenetic conditions (approximately 100–150 °C) from the products of volcanic eruptions of disputed sources and distances during the Late Devonian time.

Key words: Devonian, tephra, K-bentonite, illite, diagenesis, NW Turkey

1. Introduction

The products of explosive eruptions in the form of volcanic ash (tephra), after being transported for long distances by wind, are settled and altered to bentonites (smectite-rich volcanogenic clay rocks) in early diagenesis. In late diagenesis, these bentonites are transformed into K-bentonites by chemical modification and K-fixation with progressive illitization and then finally into metabentonites by low-grade metamorphism (Fortey et al., 1996). During diagenesis and very low-grade metamorphism, due to potassium enrichment, smectite transforms to mixed-layer illite-smectite (I-S) and then illite in K-bentonites (Weaver, 1953; Nadeau et al., 1985; Merriman and Roberts, 1990).

The discovery of K-bentonites dates back as early as the 1920s. Since then, their geologic importance has been revealed and proven by ongoing interdisciplinary research. Nelson (1921, 1922) originally denoted the pyroclastic nature of some rocks in the Paleozoic rock system in the eastern part of the United States. Following Nelson's original remarks, Allen (1932), based on the crescent-shaped shard structures and the presence of sanidine, apatite, and euhedral zircon crystals, evidenced the volcanic origin of those deposits. Rosenkrans (1934) and Kay (1944a, 1944b) were the first to use bentonites for stratigraphic correlations. The significance of K-bentonites as widespread marker beds has been recognized recently since they are also datable using fission track and U/Pb dating of zircons, K/Ar, and Ar/Ar of amphibole, biotite, and sanidine (Kolata et al., 1996).

Worldwide research activities on K-bentonites have diversified aims such as discovering localities and studying their mineralogical, petrographic, and

* Correspondence: obozkaya@pau.edu.tr

chemical properties and stratigraphic descriptions; using K-bentonite beds having event-stratigraphic significance for regional correlations; allowing the determination of paleogeographic, tectonic, and magmatic setting of source volcanoes in the studied regions; and using K-bentonites for understanding the illitization mechanism and age of illitization of smectite during burial diagenesis.

Previous investigations showed that for the explanation of the tectonic setting and genesis of K-bentonites magmatic and tectonic discrimination diagrams can be utilized (Winchester and Floyd, 1977; Floyd and Winchester, 1978; Huff and Türkmenoğlu, 1981; Merriman and Roberts, 1990; Huff et al., 1992). Although extensive research results have been published worldwide on K-bentonites of volcanic origin, only a few short reports on the occurrence of them in Turkey have been published recently (Türkmenoğlu, 2001; Türkmenoğlu et al., 2009). Those authors reported greenish-gray clay beds of 2–50 cm thick alternating with platform-type limestones and dolomitic limestones of Middle Devonian-Lower Carboniferous age in the Yılanlı Formation, which is exposed in the Zonguldak-Bartın area of the western Black Sea region. The purposes of this present study are to document the geographic and stratigraphic features of a set of K-bentonite beds in the Bartın-Zonguldak area, to summarize their clay mineralogy to help in the understanding of the diagenetic processes controlling their formation, to summarize their chemical composition to reveal original chemical characteristics of the volcanic ash from which these K-bentonites were derived, and, finally, to correlate the studied K-bentonites with data from coeval tephra worldwide.

2. Regional geological setting

The study area is located in the Bartın-Zonguldak area, in northwestern Anatolia (Figure 1a), where a set of K-bentonite beds were detected for the first time in Turkey. A set of thin K-bentonite beds were found to intercalate with the limestone and dolomitic limestone succession of the Middle Devonian-Early Carboniferous Yılanlı formation. Göncüoğlu and Kozur (1998, 1999), Göncüoğlu and Kozlu (2000), and Yanev et al. (2006) suggested that the northwestern Black Sea region comprises a terrane assemblage and consists of two different Gondwanan microplates (e.g., Göncüoğlu et al., 1997), the İstanbul terrane (İT) in the west and the Zonguldak terrane (ZT) in the east (Figure 1b). The main difference between the ZT and İT was explained by stratigraphic variations between the two and the presence of a Caledonian time thermal event in the ZT (Bozkaya et al., 2012). In the ZT, Paleozoic successions include a low-grade angular unconformity (Figures 1c and 2) between Wenlock graptolitic shales (Sachanski et al., 2010) and late Early Devonian (Emsian) (Göncüoğlu et al., 2004) carbonates, whereas in the İT, the deposition is continuous during the same time interval.

Equivalents of the studied K-bentonites were not yet described from the other parts of the İstanbul-Zonguldak terranes or their equivalents in the surrounding Paleozoic terranes such as Moesia, the Balkans, or the Caucasus. However, it may be suggested that these tephra layers were formed in relation with arc-volcanism, generated by the closure of the Variscan Rheic Ocean (Nzegge et al., 2006; Okay et al., 2010; Bozkaya et al., 2012).

A generalized lithostratigraphic section of the Zonguldak terrain is shown in Figure 2. The basement rocks are composed of a crystalline series covering continental crust-originated gneisses; an oceanic set of gabbros, basalts, and ultramafics; and an island-arc complex of pyroclastics, granites, and felsic volcanic rocks. This Cadomian basement is overlain unconformably by Lower Ordovician (Göncüoğlu et al., 2014) units, comprising greenish gray siltstones and mudstones (Bakacak Formation) and dark-red conglomerates and sandstones (Kurtköy and Aydos formations). A successive thick Upper Ordovician to Middle Silurian package is represented by the Karadere, Ketencikdere, and Fındıklı formations including graptolitic black and gray shales and siltstones with limestone interlayers (Dean et al., 1997). The Upper Silurian strata are eroded. The Fındıklı Formation is unconformably overlain by the Middle Devonian Bıçkı and Ferizli formations consisting of red sandstones-mudstones and shales-siltstones, respectively. The Late Middle Devonian-Late Early Carboniferous (Sephukovian) Yılanlı Formation, including shallow-marine dolomites and limestones, succeeds the Ferizli Formation (Aydın et al., 1987; Derman, 1997; Yalçın and Yılmaz, 2010; Bozkaya et al., 2012). The Yılanlı Formation is composed of gray, dark gray, and black medium to thick-bedded limestones, dolomitic limestones, and dolomites alternating with thin-bedded, black, calcareous shales. The approximate thickness of the Yılanlı Formation is 800 m. The transitional boundaries of the Yılanlı Formation with the Ferizli and Madendere formations were reported by Gedik et al. (2005). The fossil findings (Dil, 1976) indicate Eifelian-Visean age (Middle Devonian-Early Carboniferous) for the Yılanlı Formation. The deposition of the Yılanlı Formation continued from the Middle Devonian to Early Carboniferous in an epeiric carbonate platform/shelf (Yalçın and Yılmaz, 2010) that was covering waste areas during this time interval (Harries, 2009; Kabanov et al., 2010). The formation is overlain by a sequence of more than 500 m thick of alternating limestones and shales (Figures 1c and 2, Madendere and Karadon formations), followed by flood-plain deposits with numerous coal-stems of Westphalian age (Kerey, 1984).

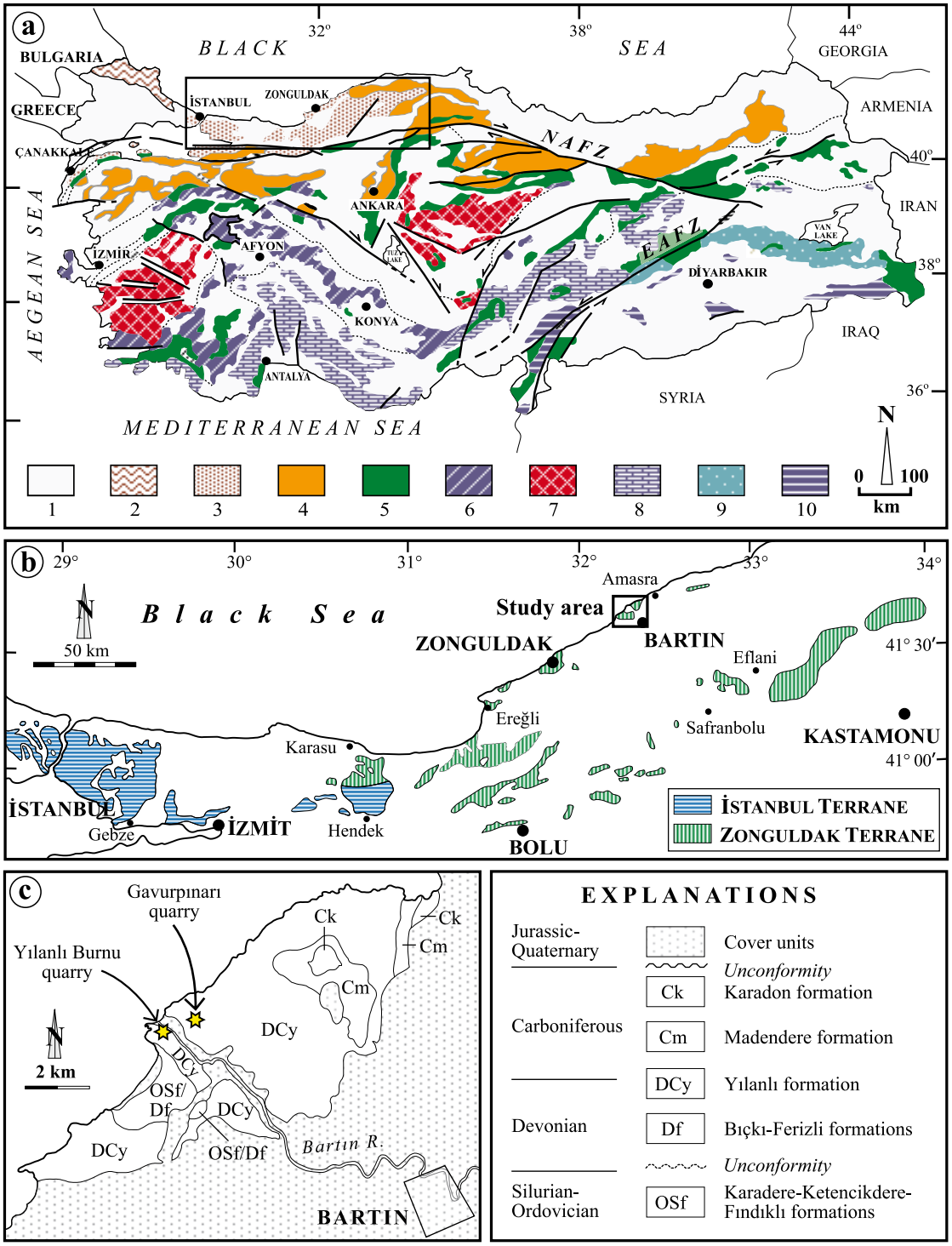

Figure 1. (a) The main tectonic units of Turkey and the location of the İstanbul and Zonguldak terranes (Göncüoğlu et al., 1997). NAFZ: North Anatolian Fault Zone, EAFZ: East Anatolian Fault Zone. Symbols: 1: Tertiary cover: 2: Istranca Terrane, 3: İstanbul-Zonguldak Terrane, 4: Sakarya Composite Terrane, 5: ophiolites and ophiolitic mélanges of Neotethyan Suture Belts, 6: Kütahya-Bolkardağ Belt (Anatolides), 7: Menderes and Central Anatolian Crystalline Complexes (Anatolides), 8: Taurides, 9: Bitlis-Pötürge Metamorphics (SE Anatolian Autochthon), 10: SE Anatolian Autochthon. **(b)** The distribution of the Paleozoic outcrops in the İstanbul and Zonguldak terranes (modified from Bozkaya et al., 2012). **(c)** Geological map of the study area and geographic settings of sampling quarries (modified from Akbaş et al., 2002).

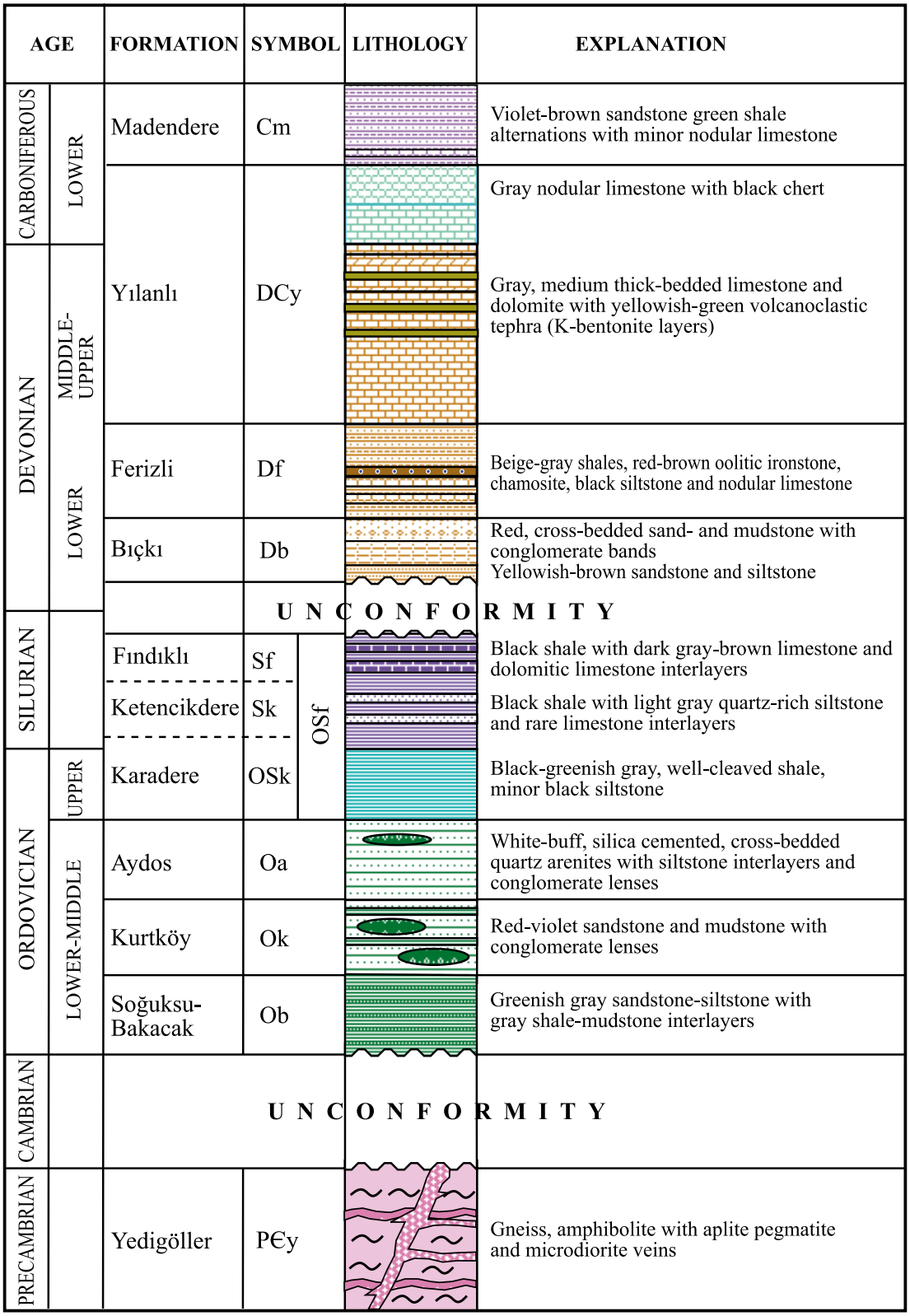

Figure 2. Generalized lithostratigraphic section of the Zonguldak terrain (modified form Bozkaya et al., 2012).

The oldest cover of the Variscan units of the Zonguldak Terrane are the Upper Permian (Tatarian) lagoonal sediments (Göncüoğlu et al., 2011) to Upper Triassic continental red beds of the Çakraz Formation (Alişan and Derman, 1995).

3. Stratigraphy of the K-bentonite beds

The studied K-bentonite beds are found in the upper part of the Yılanlı Formation in the ZT. K-bentonites outcrop mainly at two areas to the north of Bartın. The first outcrop, the Gavurpınarı limestone quarry, is located around Gavurpınarı, to the north of Bartın (Figure 1c). It is included within the 1:25,000-scale E28c1 map of Turkey, with the coordinates of 41°42'04.39'N, 32°1'41.88'E. The second outcrop is at the Yılanlı Burnu quarry to the northwest of Bartın Çayı, on the Black Sea coast. This area is located within the 1:25,000-scale E28d2 map at 41°41'05.10'N, 32°14'49.60'E.

At the Gavurpınarı quarry, a 40-m-thick package of the Yılanlı formation is exposed (Figure 3). The layering of the limestones in the quarry is almost vertical. The studied section is at the northernmost edge of the third quarry level. Here, the section starts at a fault within the Yılanlı formation. Towards the south, it comprises massive, gray-brown limestone-dolomitic limestone layers, interbedded with a set of K-bentonite beds with thicknesses varying between 2 and 60 cm (Figure 3). K-bentonites characteristically have blue-green colors when fresh but they became yellowish brown in color due to weathering. When wet, they have a waxy, slippery texture due to their clay-rich composition.

At the Yılanlı Burnu quarry, the Yılanlı formation is 46 m thick and exposed as alternations of limestone, dolomitic limestone, marl layers, and thin clay beds (Figure 4). Limestones are cream-gray in color and have bioclastic, peloidal, and fossiliferous textures. They are highly dolomitized and affected by intensive folding and faulting. A number of green-gray K-bentonite beds are exposed, intercalated with carbonate rocks at the lowermost part of the sequence (Figure 4).

K-bentonite beds do not include any organic material and hence they were dated indirectly by the fossils found within the limestones underlying and overlying them. The marly limestones below the bentonitic beds include bands of a few millimeters in thickness, very rich in ostracods. The ostracods and the very few conodonts that we found were not enough to yield reliable ages. However, the pure limestones between the K-bentonites in the Gavurpınarı limestone quarry (see Figure 3) included foraminifera such as *Parathurammina elegans* Poyarkov, 1969; *Bisphaera elegans* Vissarionova, 1950; *Radiosphaera* spp.; *Tubeporina* sp.; *Elenella* sp.; *Irregularina* spp.; *Eogeinitzina* sp.; and *Eogeinitzina* (?) spp. From these, the age-diagnostic taxon is *Eogeinitzina* sp., which is indicative for the Frasnian and mainly the late Frasnian (Dil, 1976; Vachard, 1991, 1994; Vachard et al., 1994; Racki and Sobon-Podgorska, 1993; Kalvoda, 2001; Sabirov, 2004).

4. Materials and methods

A total of 46 samples were collected from the Gavurpınarı and Yılanlı Burnu quarries for laboratory analysis. Mineralogical properties were investigated by polarizing microscope, scanning electron microscope equipped with energy dispersive X-ray spectrometry (SEM-EDX), X-ray powder diffractometer (XRD), and high-resolution transmission electron microscopy (HR-TEM) in the Central Laboratory of Middle East Technical University. Chemical analyses of the samples were conducted by inductively coupled plasma-mass spectrometry (ICP-MS) by ACME Analytical Laboratories Ltd. (Vancouver, Canada).

The bulk and clay mineralogy and the crystal-chemical data of illites were studied for 14 samples by XRD using a Rigaku Miniflex II diffractometer with Ni-filtered CuKα radiation and a graphite monochromator. The X-ray tube was operated at 35 kV and 15 mA with a scanning speed of 2° 2θ/min for mineral identification and 1° 2θ/min for illite crystal-chemical characteristics (e.g., illite crystallinity; Kisch, 1991; Histon et al., 2007). Clay fractions (grain size of <2 μm) were separated by dispersing the bulk sample in distilled water after acid treatment to eliminate carbonate minerals, followed by sedimentation and centrifugation. Oriented mounts were obtained by thin-smeared clay paste on glass slides. Similar procedures were used to further fractionate the clay fractions into finer grain sizes (1–2 μm, 0.5–1 μm, 0.25–0.5 μm, <0.25 μm). XRD patterns were obtained for air-dried, ethylene-glycolated samples that were heated at 350 and 550 °C. For the determination of clay minerals from XRD patterns, the data of Hoffman and Hower (1979) and Moore and Reynolds (1997) were used. Illite "crystallinity" (Kübler index, KI; Kübler, 1968; Guggenheim et al., 2002) was determined by measuring the full width at half maximum (FWHM) at the first basal illite reflection near 10 Å in air-dried samples. Crystallinity index standards (CIS; Warr and Rice, 1994) were used for calibration of FWHM values to KI with the linear equation of $IC_{CIS} = 1.18 \times IC_{ODTU} - 0.015$, $r^2 = 0.999$. Narrowing of the peak width suggests an increase in crystallinity due to a decrease of the scattering domain of illite by collapse of interlayers and conversion of smectite to illite under increasing temperature and pressure conditions. A broad peak indicates interstratification of expandable clays, interlayer hydration, and small crystal size (Weaver, 1961; Kübler, 1968). Three main zones, a low- and high-grade diagenetic zone (0.42), anchizone (0.42-0.25), and epizone (< 0.25), were distinguished for KI values (e.g., Frey, 1987;

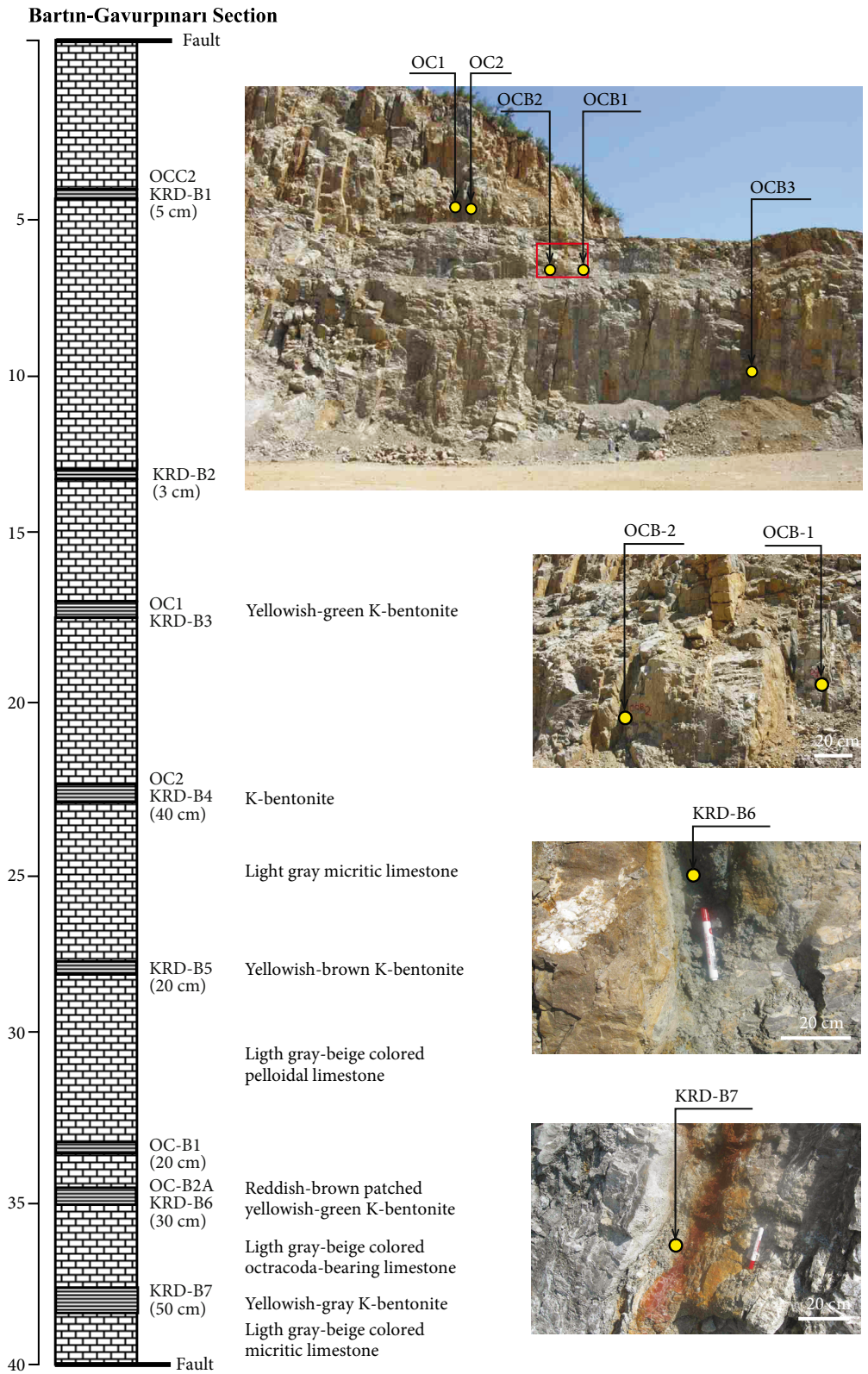

Figure 3. Stratigraphic distribution, field appearance, and sample locations (yellow spots) of K-bentonite layers in the Gavurpınarı limestone quarry.

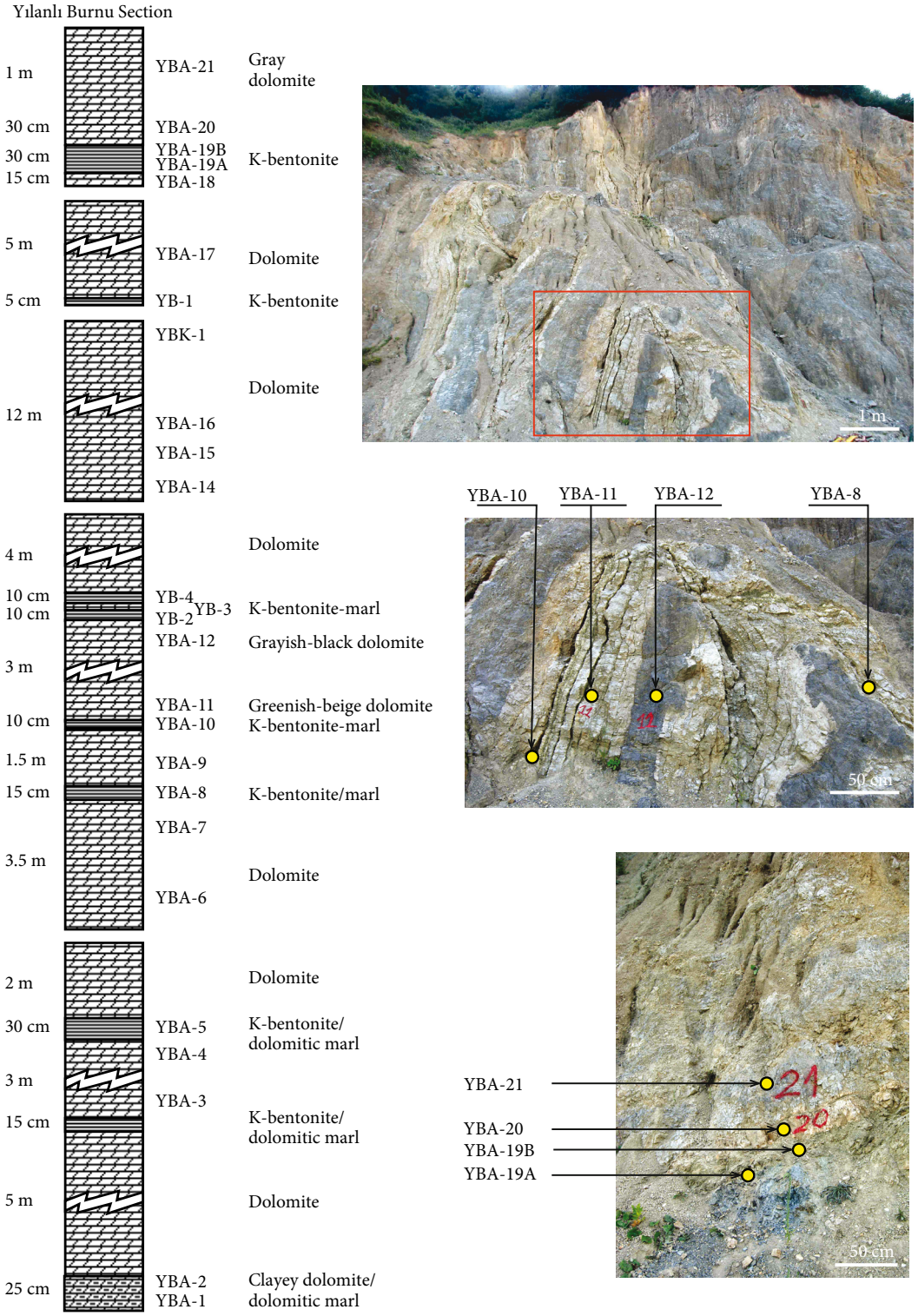

Figure 4. Stratigraphic distribution, field appearance, and sample locations (yellow spots) of K-bentonite layers in the Yılanlı Burnu quarry.

Merriman and Frey, 1999). The intensity ratio [Ir = (I001)/$(I003)_{air\text{-}dried}$ / (I001)/$(I003)_{ethylene\text{-}glycolated}$)] measurements were realized for the relative abundance of expandable (smectite) layers (Środoń, 1984). The d_{060} values of illite were identified for estimating the octahedral Fe+Mg content (atoms per formula unit, a.p.f.u.) of illites by using the equation of Hunziker et al. (1986). Illite crystallite size (domain size) values were estimated on the KI-Ir diagram of Eberl and Velde (1989) and checked by data obtained from the WINFIT computer program (Krumm, 1996). The deconvolution of XRD patterns was also performed using this computer program. Illite polytypes were identified at characteristic peaks (2θ = 16°–36°) for unoriented preparations (Bailey, 1988). $I_{(2.80)}$ / $I_{(2.58)}$ and $I_{(3.07)}$ / $I_{(2.58)}$ peak area ratios, proposed by Grathoff and Moore (1996), were used in order to identify polytype ratios.

The SEM-EDX studies were performed using a Quanta 400F field emission instrument in order to determine the particle morphologies and textural relationships. Operating conditions were arranged as 32 s counting time and 20 kV accelerating voltage. Additionally, the chemical data were obtained by EDX. HR-TEM was used to observe the clay mineral structures in detail. For this purpose, clay fractions of <0.1 μm were separated by a high-speed centrifuge and then examined with HR-TEM using a JEOL JEM 2100F instrument operating at 80–200 kV on samples precipitated from a dilute suspension onto a carbon-coated grid in order to examine lattice images and thickness distribution of illites.

5. Results

5.1. Optical microscopy

K-bentonites collected from different beds at the Gavurpınarı and Yılanlı Burnu quarries display similar mineralogical and petrographic features (Figure 5). The relict primary minerals characterizing the volcanic origin of those K-bentonites are biotite, zircon, quartz, feldspar, amphibole, and apatite. Biotite and zircon crystals display euhedral to anhedral crystal outlines. The vitroclastic pyroclastic texture including completely sericitized (illitized) volcanic matrix, volcanic glass, and/or pumice shards (Figures 5a and 5b) and the presence of euhedral zircon and biotite crystals indicate volcanic origin for K-bentonites. However, some zircon crystals are slightly rounded (Figures 5c and 5d), which is attributed to their detrital origin. The crystal size of idiomorphic zircons is about 100 μm, which indicates a distal volcanic source for parent tephra. Pyrite, dolomite, gypsum, and calcite formed as diagenetic minerals. Pyrites are mostly oxidized to limonite, which resulted in the yellowish-brown colors of K-bentonites in field exposure. At Yılanlı Burnu quarry, dolomite and very fine-grained sericitized materials are found together, and therefore K-bentonites exhibit some differences as tuffite or dolomitic marls (Figures 5e and 5f).

The carbonate rocks at the Gavurpınarı quarry consist of stromatolite-bearing dolomitic limestones, ostracod-bearing peloidal micritic limestones, ostracod-bearing clayey limestones, ostracod- and intraclast-bearing peloidal micritic limestones, polygenic calcareous breccia, and clayey limestone/marl. At the Yılanlı Burnu quarry, the main lithologies are composed of limestones or dolostones, where dolomitization is more intensive compared to the Gavurpınarı samples. Rhombohedral dolomite crystals can be observed as replacing calcite. Dolomitized stromatolite, bivalve-bearing dolostone, peloidal dolostone, organic dolostone, and ostracod-bearing clayey limestone/marl facies are common at this location.

Both field observations and microfacies distribution demonstrate the abundance of stromatolite- and ostracod-bearing facies contrary to the absence of any pelagic and/or sedimentary structures indicating a high-energy environment characteristic of a shallow intraplatform sedimentation environment. Additional supporting evidence is the presence of microbreccia and the absence of coral/crinoid/echinoid/foraminifera/algae fossils. All together the successive intercalation of marl and mudstone (or tephra) and limestone and dolostone indicates that the sedimentation environment should be an 'epeiric' platform.

5.2. Clay mineralogy

Illite is the major clay mineral in the K-bentonite samples from the two quarry locations (Figure 6). In a few samples, kaolinite and mixed-layer illite/smectite are also identified. Trace quantities of imogolite could be detected by its 18 Å peak in the very-fine size fraction (<0.5 μm) of samples OCB-2 and YBA-19A from the Gavurpınarı and Yılanlı Burnu quarries, respectively (Figures 7 and 8). This mineral is known from modern soils that have formed from volcanic tephra, and it is generally not preserved in sedimentary deposits. The existence of negligible amounts of imogolites should be related to soil formation processes. Illites have typical sharp peaks at 10 Å (001), 5 Å (002), and 3.33 Å (003) indicating pure illite. However, the deconvolution of asymmetric peaks as performed by the WINFIT program shows the presence of phases of well-crystallized illite (WCI), poorly crystallized illite (PCI), and lesser amounts of mixed-layer illite-smectite (I-S) (Figure 9). Together with the increasing crystal sizes from <0.25 μm to >2 μm, the PCI and WCI peaks relatively sharpen and become narrower, in accordance with a progressive diagenetic process. During progressive diagenesis, the percentage of the mixed-layer I-S subpopulation decreases, while the abundance of PCI and especially WCI increases (Lanson et al., 1998; Bozkaya et al., 2011).

The KI values of illites range from 0.69 to 0.77 (average:

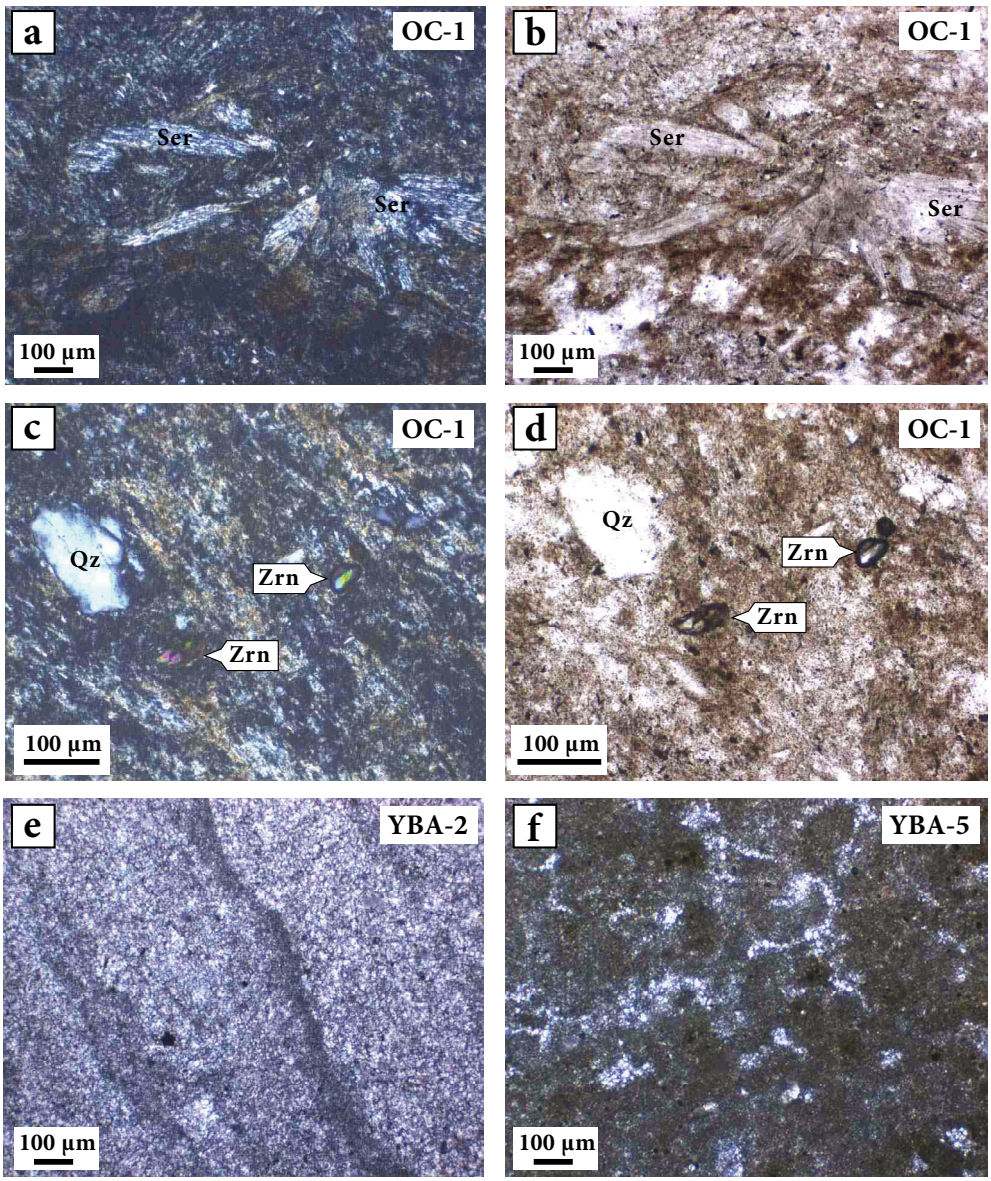

Figure 5. Photomicrographs of K-bentonite samples. **(a, b)** Pyroclastic (vitroclastic) textured K-bentonite sample from Gavurpınarı quarry with sericitized volcanic matrix and shards of glass (or pumices) of **a**-crossed nicols-*cn*, **b**- plain polarized light-*ppl*. **(c, d)** Sub- to anhedral and slightly rounded subhedral zircon crystals within the sericitized volcanic matrix of K-bentonite sample from Gavurpınarı quarry, **c**-*cn*, **d**- *ppl*. **(e)** Very-fine-grained sericitized materials and fine-grained dolomites in the dolomitic tephra (tuffite) in the Yılanlı Burnu quarry (*cn*). **(f)** Dolomite-rich tephra with low amounts of sericitized volcanic materials in the dolomitic marl in the Yılanlı Burnu quarry (*cn*).

0.72 Δ°2θ) for Gavurpınarı quarry samples and 0.47 and 0.93 (average: 0.71 Δ°2θ) for Yılanlı Burnu quarry samples, indicating high diagenetic grade (Table 1; Figure 10). Although these values are similar for both quarries, illites in the Yılanlı Burnu quarry reflect a somewhat higher grade than the Gavurpınarı area. In terms of phyllosilicate reaction series in clayey rocks, KI values reflect progressive reactions such as the depletion in smectite layers, a decrease in compositional heterogeneity of series members, and polytypic transformations during the illitization process. It is primarily controlled by parameters such as disorder in crystal structure, crystal thickness, crystal size, expandable mineral presence, precursor volcanic glass composition, and stage of diagenesis during illitization (Altaner and Ylagan, 1997).

The *Ir* values (1.26–1.53, an average of 1.42 for the

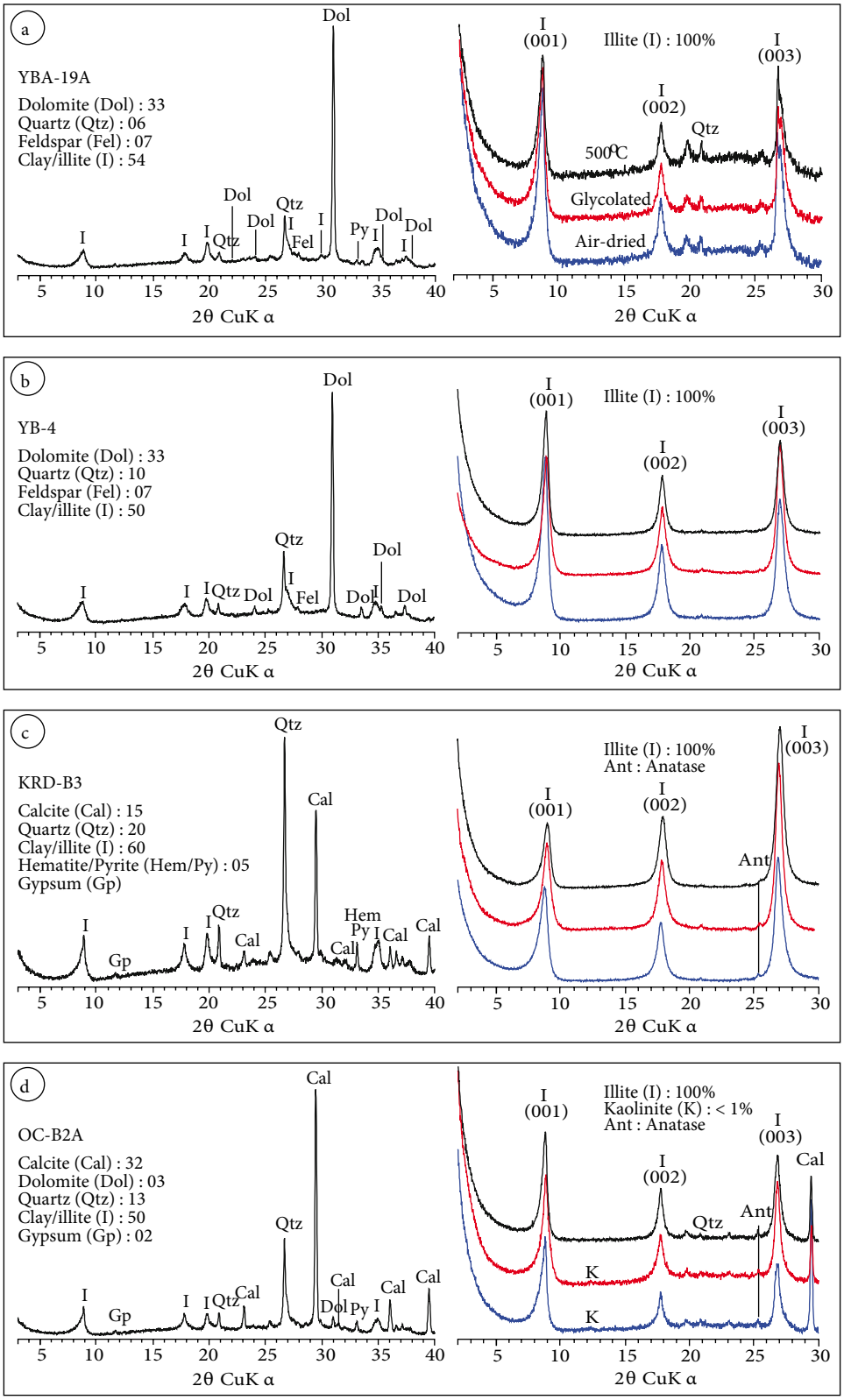

Figure 6. XRD patterns of bulk and oriented clay fractions of samples from Yılanlı Burnu (YBA-19A and YB-4) and Gavurpınarı (KRD-B3, OCB-2A) quarries.

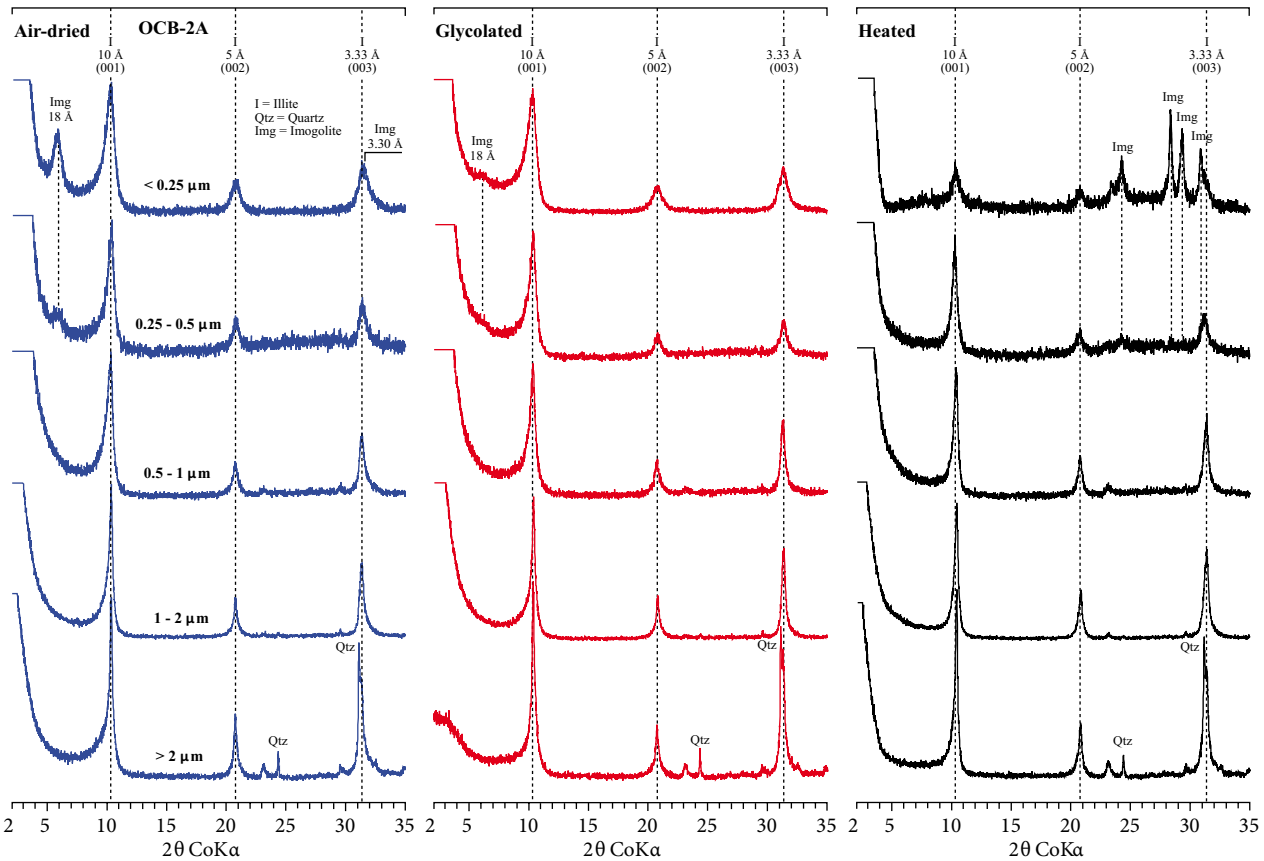

Figure 7. The variations of XRD patterns of clay fraction according to different sizes in OCB-2A sample from Gavurpınarı quarry.

Gavurpınarı quarry, and 1.13–1.44, an average of 1.32 for the Yılanlı Burnu quarry) point to the presence of swelling layers (smectite) in illites. Thus, *Ir* values of Gavurpınarı illites display higher values than Yılanlı Burnu quarry illites, which can be explained by relatively higher smectite contents and lower diagenetic conditions. The comparison of KI and *Ir* values of illites indicates that the content of swelling (or smectite) component and crystallite sizes (*N*) of illites are 2%–5% and 10–25 nm, respectively (Figure 10). The determined illite polytypes in K-bentonites are $2M_1$ and $1M_d$ (Figure 11). The $2M_1/(2M_1 + 1M_d)$ ratios (%) are more or less similar (20%–50%, an average of 37%) for the two quarries; however, illites of the Yılanlı Burnu quarry have more $2M_1$ than illites of the Gavurpınarı quarry (Table 1). Based on the d_{060} reflections (1.4991–1.5033 Å), the octahedral Mg+Fe contents of illites are between 0.27 and 0.48 a.p.f.u., showing the dioctahedral composition between end-member muscovite and phengite.

5.3. Micromorphology and crystal structures of illites

Illites belonging to K-bentonites from the Gavurpınarı and Yılanlı Burnu quarries exhibit a platy habit with curved edges (Figure 12a). Nadaeu et al. (1985), Inoue et al. (1990), and Altaner and Ylagan (1997) stated that this kind of platy morphology with anhedral flakes is a common feature for illites from K-bentonites. By increasing the proportion of illite layers in mixed-layer I-S, the morphology of illite changes from sponge-like or cellular to platy or ribbon-like as a result of a change in layer stacking from turbostratic (randomly distributed layers in any direction) to rotational ordering of the $1M_d$ type during burial diagenesis. This rotationally ordered structure results in a plate or sheet-like crystal habit by means of the contiguity of quasihexagonal oxygen surfaces from adjacent layers, which allows more crystalline regularity in the direction of the *a*-*b* plane (Keller et al., 1986).

The <0.1 µm size fractions of the clay illite from K-bentonite samples from two different locations were investigated by HR-TEM. Regular stacking sequences of illites could be observed (Figure 12b). It is suggested that the illite mineral can be a long-range ordered (≥R3) mixed-layer illite-smectite on the basis of change from random (R0) to short-range (R1) ordered, and then to long-range (R3) ordered I-S during progressive illitization of smectite (e.g., Bethke et al., 1986; Lindgreen and Hansen, 1991). Illite crystals exhibit anhedral lamellar micromorphologies

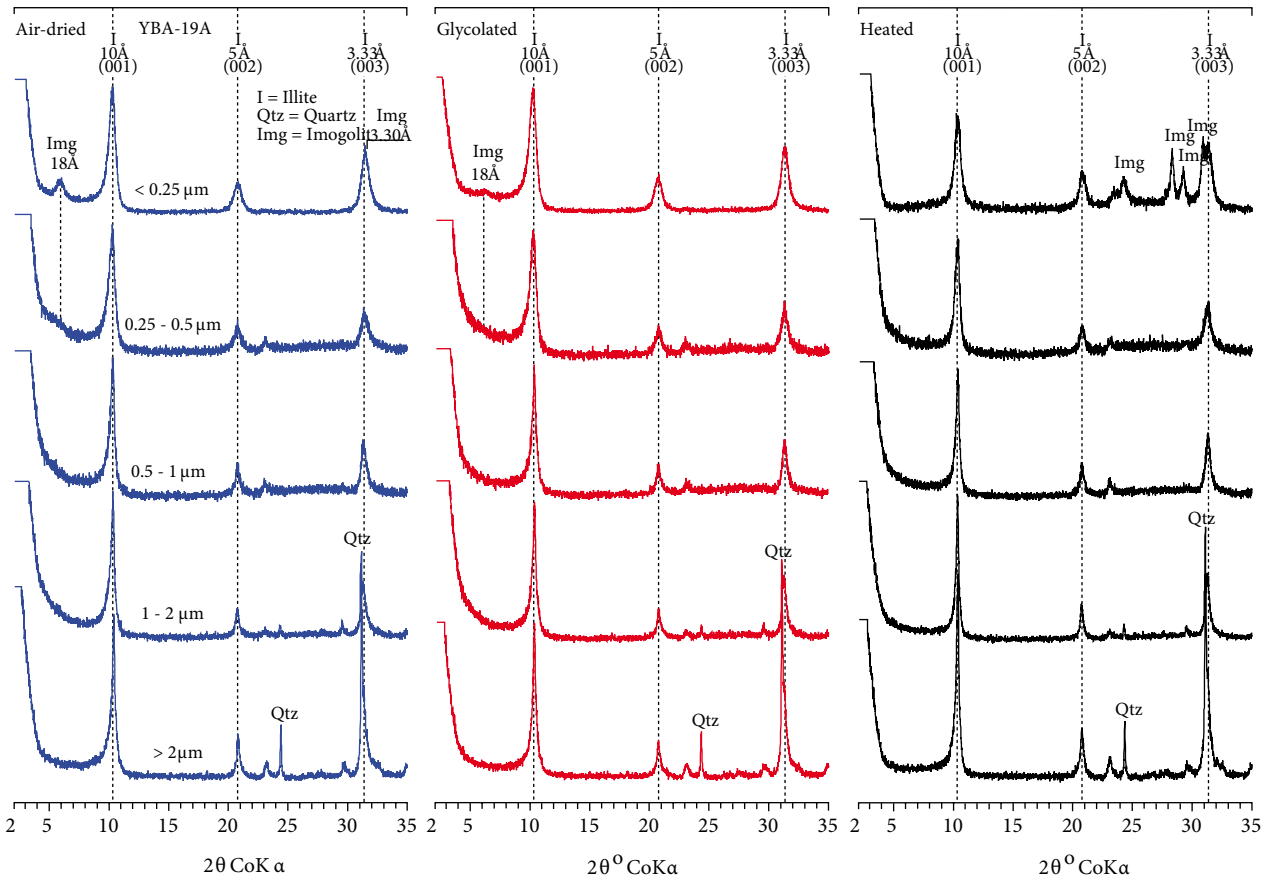

Figure 8. The variations of XRD patterns of clay fraction according to different sizes in YBA-19A sample from Yılanlı Burnu quarry.

and ordered lattice fringe images with T-O-T layers (Figure 12b). This kind of ordered structure without any defects demonstrates an effect of the advanced stage of diagenetic evolution on the studied illites (Merriman and Peacor, 1999). The crystallite sizes of illite particles reach up to 20 nm, compatible with data obtained from the KI-*Ir* diagram (see Figure 10).

5.4. Chemical composition of tephras

Depending on the composition of the precursor tephra and the water/rock ratio in a marine system, the chemical composition of the initial ash is modified through gains and losses of elements with respect to the altering solutions (Christidis, 1998). During diagenesis, by homogenization of tephra with marine and pore water, volcanic glass progressively alters or transforms into smectite, then mixed-layer illite-smectite, and finally illite. Thus, in this study, the major elements are not considered in determination of original volcanic ash composition due to modification of their relative proportions by alteration processes. Thus, only the less mobile trace element- and rare earth element-based chemical classification (Winchester and Floyd, 1977) are utilized in order to reveal the original compositions of the precursor tephras. The geochemical properties of K-bentonites also provide information on the tectonomagmatic settings of eruption centers as the sources of these tephras.

In Tables 2 and 3, the bulk chemical analysis results of K-bentonites and K-bentonite-bearing carbonate rock samples from the Gavurpınarı and Yılanlı Burnu quarries are listed, respectively. In general, as the CaO and MgO values increase due to the presence of calcite and dolomite, the SiO_2 and Al_2O_3 concentrations decrease. High Fe_2O_3 contents occur because of abundant pyrite of secondary origin. The K_2O values, which reach up to 6%, indicate the dominancy of illite in K-bentonites.

The Zr/TiO_2 - Nb/Y immobile trace element diagram (Figure 13) is useful to determine the source characteristics of the tephra (Floyd and Winchester, 1978). Plotting of eight K-bentonite samples on this diagram demonstrates that the precursor volcanic ash(es) had an alkali-basaltic character (Chalot-Prat et al., 2007).

The samples from both the Gavurpınarı and the Yılanlı Burnu quarries display similar geochemical trends based on chondrite-normalized trace and REE diagrams. However,

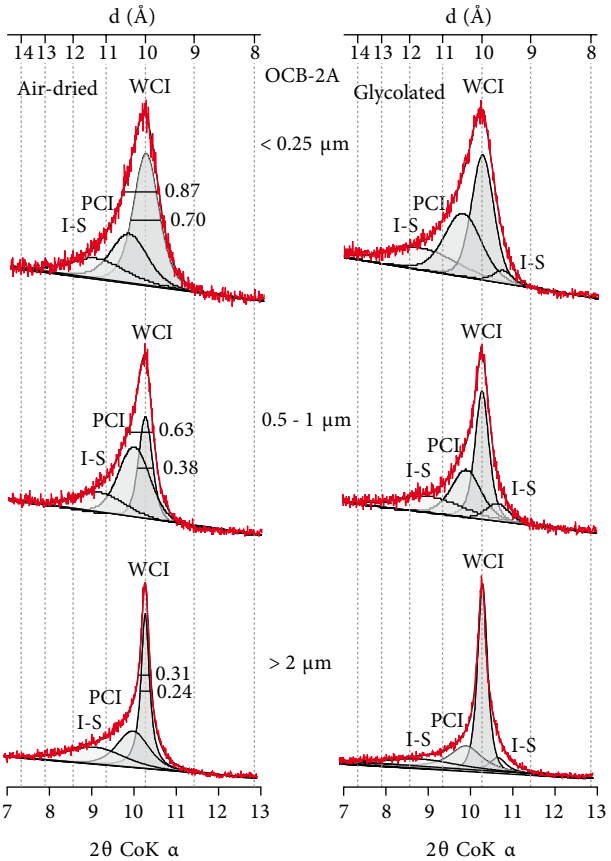

Figure 9. Decomposition of first basal illite peaks near 10 Å for different size fractions and variations in peak widths in OCB-2A sample from Gavurpınarı quarry (WCI = well-crystallized illite, PCI = poorly crystallized illite, I-S = illite-smectite).

Table 1. The crystal chemical properties of illites.

Sample no.	Quarry	KI(Δ°2q)	I_{002}/I_{001}	Ir	d_{060}	*b*	$1M_d$	$2M_1$	Mg/Fe
OCB1-S	Gavurpınarı	0.69	0.38	1.53	1.5015	9.0090	55	45	0.39
OCB2-A	Gavurpınarı	0.69	0.38	1.26	1.5000	8.9990	60	40	0.32
OC2B-B	Gavurpınarı	0.77	0.40	1.48	1.4991	8.9946	75	25	0.27
KRD-B6	Gavurpınarı	0.74	0.49	1.42	1.4996	8.9976	35	65	0.30
YB-1	Yılanlı Burnu	0.47	0.37	1.43	1.5013	9.0078	60	40	0.38
YB-2	Yılanlı Burnu	0.78	0.41	1.13	1.4995	8.9970	80	20	0.30
YBA-5	Yılanlı Burnu	0.53	0.43	1.20	1.5039	9.0234	50	50	0.51
YBA-8	Yılanlı Burnu	0.93	0.48	1.44	1.4992	8.9952	80	20	0.28
YBA-10	Yılanlı Burnu	0.84	0.40	1.38	1.5013	9.0078	55	45	0.38
YBA-19A	Yılanlı Burnu	0.69	0.32	1.32	1.5033	9.0198	60	40	0.48

the tephras of the Gavurpınarı quarry are relatively more enriched than tephras of the Yılanlı Burnu quarry (Figures 14 and 15). The lack of negative anomalies of Ta and Nb elements and the REE diagram indicate a possible mantle source for the tephras. The relative negative anomaly of Sr can be explained by alteration of the bentonites. The negative Eu anomaly is commonly attributed to the removal of Eu by plagioclase during fractionation of the

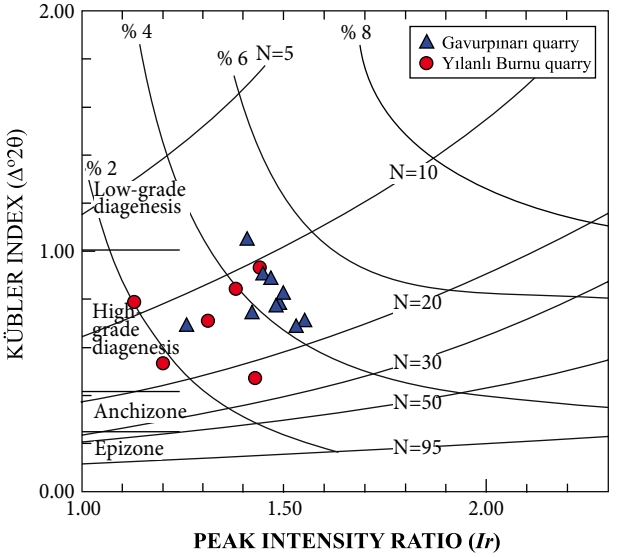

Figure 10. Diagenetic grade, smectite contents, and crystallite size of illites on KI versus *Ir* diagram of Eberl and Velde (1989).

melt. This anomaly is typical of evolved magmas (Calarge et al., 2006). K in illite compositions could be sourced from K-bearing primary igneous minerals such as feldspars or micas. However, for the original composition of volcanic material generating those studied K-bentonites (tephras), the geochemical discrimination analyses suggest an alkali-basaltic magma source (Figure 13), and an anorthite-rich feldspar composition will be expected for this magma composition. Thus, the possible source of the high K content of illites remains a question.

6. Discussion

6.1. Mineralogy and depositional environment

K-bentonites intercalated with the carbonate rocks of the Late Devonian-Early Carboniferous Yılanlı formation exposed at the Gavurpınarı and Yılanlı Burnu quarries consist mainly of illite, although some kaolinite and mixed-layer illite-smectite is also present. The major nonclay minerals of primary volcanic origin are quartz, feldspar, biotite, zircon, and apatite. This assemblage of nonclay minerals detected in K-bentonites is a strong indication of parent volcanic ashes (tephra), which are probably from a distal volcanic source as suggested by very small crystal size of around 100 m.

New minerals, which are foreign to the original tephras, are the clay minerals illite, kaolinite, and mixed-layer I-S. They owe their origin to the diagenetic processes. Pyrite, calcite, dolomite, and gypsum, on the other hand, are the new nonclay minerals, formed also due to diagenetic processes. Pyrite is present abundantly in some of the K-bentonite samples. They were oxidized when exposed to air so that the original grayish-green colors of K-bentonite beds turned to brownish. This property provides a quick identification of K-bentonites beds in the field.

The petrographic examination of carbonate rocks, mainly limestones and dolomitic limestones, from the studied quarries indicated that the original volcanic ashes were settled in a shallow intraplatform depositional environment. Intercalating mudstone and marl with limestone and dolostone lithologies in the studied quarries defines an "epeiric" platform character for the sedimentary depositional environment. In such an environment, interaction between deposited ash and seawater should cause very early diagenesis of ash (halmyrolysis) on the sea bottom and should cause elemental gains and losses, especially in the major elemental compositions of the original tephras.

6.2. Illitization process and degree of diagenesis

Crystal-chemical data (KI, polytypes, d_{060}), SEM observations, SEM-EDX data, and HR-TEM studies of K-bentonites reveal similar characteristics for both quarries. The polytype ratios, the Mg+Fe content of dioctahedral layers, the platy morphology of illites, the presence of zircon and biotite minerals, and the ordered layer structures of illites support the idea that K-bentonites formed as a consequence of illitization of tephras under high-grade diagenetic conditions (100–150 °C). Very low (5%) smectite content of the clay mineral fraction of K-bentonites indicates the alteration of volcanic glass to smectite at early stages of diagenesis and with progressive diagenetic transformation; thus, illite became dominant in K-bentonites. Polytype identification of the illites from the Gavurpınarı and Yılanlı Burnu K-bentonites indicated that no significant differences exist between the two locations, and so the diagenetic conditions affecting both areas of deposition are similar. Illite polytypes identified for different size fractions showed that K-bentonites formed by progressive diagenetic maturation: with increasing crystallite size of illites, $1M_d$ polytypes were replaced by the $2M_1$ polytype due to increasing grade of diagenesis.

6.3. Chemistry of K-bentonites and source of volcanism

The parental ash compositions of K-bentonites are deduced from trace and REE data by means of chemical discrimination diagrams. The results obtained from them indicate that the original ashes had alkali basaltic compositions, close to the field of trachyandesite in the Zr/TiO_2 - Nb/Y diagram. This may partially explain the origin of K for illitization of smectite, which took place during diagenesis of tephras. However, the origin of potassium is still not known for the studied K-bentonites. Possible sources of K might be volcanogenic minerals like biotite or feldspars that were existing in the original ash or the seawater. In the REE diagrams, the lack of Ta and Nb negative anomalies are characteristic of a mantle origin of the original volcanic ashes forming K-bentonites by diagenetic evolution.

Table 2. Geochemical compositions of K-bentonite bulk samples from Gavurpınarı quarry.

Element	OC1	OCB2A	OCB2B	OCB1G	OCB1S	OCB3	OC2	KRDB6	KRDB7
In weight %									
SiO_2	58.64	23.35	25.93	42.18	52.85	32.33	28.65	47.75	35.91
Al_2O_3	21.5	8.93	9.76	13.71	18.53	12.27	10.93	17.99	15.26
Fe_2O_3	2.45	3.22	3.89	5.61	8.76	5.43	2.83	3.74	4.69
MgO	0.9	1.43	1.57	2	2.65	1.72	1.69	5.06	2.18
CaO	0.83	31.23	28.33	14.76	1.28	21.51	27.1	5.27	16.83
Na_2O	0.11	0.05	0.05	0.08	0.1	0.06	0.05	0.10	0.08
K_2O	2.66	2.96	3.2	4.47	6.01	3.82	3.54	5.74	4.88
TiO_2	1.2	0.45	0.5	0.68	0.94	0.57	0.57	0.88	0.78
P_2O_5	0.05	0.09	0.09	0.17	0.28	0.22	0.13	0.23	0.20
MnO	<0.01	0.01	0.01	0.01	<0.01	<0.01	<0.01	<0.01	<0.01
Cr_2O_3	0.021	0.008	0.009	0.011	0.016	0.011	0.01	0.016	0.014
LOI	11.5	28.1	26.6	16.2	8.4	21.9	24.4	13.0	19.0
Total	99.86	99.87	99.88	99.85	99.82	99.82	99.87	99.76	99.81
In ppm									
Ni	26	30	23	122	50	35	23	30	45
Sc	20	8	8	12	16	9	10	15	14
Ba	385	133	143	214	258	164	148	265	210
Be	5	2	4	4	4	2	<1	3	3
Co	2.7	9.1	4	40.4	10.8	10.1	4.3	8.2	8.2
Cs	23.1	6.6	6.6	10.4	13	6.9	7.5	12.1	17.6
Ga	24.9	9.7	11.6	16.2	23.4	13.8	13.3	22.5	17.3
Hf	6.2	2.6	2.7	3	4.6	2.3	3	4.7	4.1
Nb	21.8	10.7	12	14.8	20.6	11.8	13.2	23.8	17.5
Rb	120.2	107.2	129.5	153.3	210.1	127.7	134.7	193.5	173.2
Sn	4	2	2	2	3	2	2	3	5
Sr	75.4	377.3	267.6	197.5	171.5	733.3	330.6	268.8	502.1
Ta	1.4	0.7	0.8	0.9	1.3	0.7	0.6	1.3	1.2
Th	12.2	7.7	8.5	10.9	14.2	8.6	8.9	17.0	14.3
U	4.2	3.7	2.4	24.5	8.8	5.1	3.1	9.6	6.1
V	198	68	78	94	148	136	82	152.0	173.0
W	3.2	1.5	2.2	2.2	3.2	2.7	3.6	5.4	5.0
Zr	216.5	84.3	95.4	117.5	172.8	94.6	113.9	177.1	148.1
Y	18.7	12.4	11.3	15.4	21.6	8.1	14.5	13.3	14
La	32.3	20.1	19.2	27.1	35.6	20.4	24.1	30.3	26.8
Ce	55.2	40	40.9	56.8	76.1	39	51	66.5	60.4
Pr	6.03	4.74	4.53	6.92	9.1	4.35	6.07	6.85	6.45
Nd	21.8	16.1	15.8	25.5	33.3	15.3	22.7	24.1	22.7
Sm	3.43	3.05	2.8	4.74	6.34	2.56	4.22	4.15	4.13
Eu	0.67	0.57	0.52	0.93	1.19	0.46	0.87	0.75	0.76
Gd	2.61	2.46	2.19	3.65	5.01	1.72	3.36	3.03	3.03
Tb	0.45	0.38	0.35	0.55	0.75	0.28	0.52	0.50	0.53
Dy	3.01	2.24	2.09	2.83	4.42	1.58	2.82	2.79	2.79
Ho	0.66	0.42	0.41	0.58	0.79	0.33	0.55	0.58	0.57
Er	2.32	1.32	1.24	1.67	2.24	0.98	1.68	1.68	1.71
Tm	0.37	0.2	0.21	0.25	0.35	0.15	0.23	0.28	0.28
Yb	2.66	1.37	1.39	1.72	2.39	1.12	1.58	1.96	1.80
Lu	0.4	0.2	0.2	0.23	0.34	0.16	0.24	0.29	0.25

Table 3. Geochemical compositions of K-bentonite bulk samples from Yılanlı Burnu quarry.

Element	YB4	YBA5	YBA19A	YB1	YB2
In weight %					
SiO_2	42.4	12.41	38.74	6.82	44.26
Al_2O_3	14.32	4.09	14.35	2.04	15
Fe_2O_3	3.6	1.44	4.79	0.92	3.95
MgO	9.16	16.51	8.53	18.56	8.12
CaO	6.93	23.42	8.62	27.01	6.05
Na_2O	0.05	0.04	0.08	0.04	0.06
K_2O	5.8	1.81	5.91	0.73	5.81
TiO_2	0.44	0.19	0.42	0.11	0.62
P_2O_5	0.04	0.04	0.1	0.13	0.06
MnO	0.02	0.01	0.02	0.01	0.01
Cr_2O_3	0.01	0.004	0.011	0.003	0.012
LOI	17	39.7	18.2	43.3	15.8
Total	99.8	99.69	99.77	99.64	99.79
In ppm					
Ni	28	<20	41	<20	29
Sc	10	4	13	2	10
Ba	81	64	159	44	93
Be	3	<1	<1	<1	2
Co	8.9	2.8	10.9	2.2	6
Cs	11.5	1.8	8.5	0.8	12.6
Ga	18	4.7	17.9	2.1	21.9
Hf	2.5	1.1	1.1	0.7	3.2
Nb	9.4	3.1	7.3	1.7	12
Rb	197.2	43.6	163.8	16.8	198.7
Sn	2	<1	2	<1	3
Sr	68.1	104.6	241.6	299.7	162.6
Ta	0.6	0.2	0.5	0.2	0.9
Th	9.3	2.9	6.5	1.5	12.3
U	3.6	3.7	10.3	3.6	6.6
V	90	31	97	22	98
W	1.2	0.5	1	0.8	1.6
Zr	79.5	32.1	38.8	22.2	112.5
Y	5.4	4.2	9.7	3.9	6.1
La	14.2	6.8	20.2	4.2	20.4
Ce	23.1	14	35	8	31.8
Pr	2.46	1.62	3.94	1.01	3.24
Nd	8.4	6.1	12.9	3.6	9.7
Sm	1.28	1.23	2.64	0.71	1.52
Eu	0.2	0.23	0.53	0.14	0.24
Gd	0.87	0.91	2.25	0.61	0.95
Tb	0.14	0.15	0.34	0.1	0.17
Dy	0.82	0.81	2.04	0.66	1.27
Ho	0.2	0.16	0.38	0.12	0.22
Er	0.61	0.5	0.99	0.33	0.78
Tm	0.1	0.07	0.16	0.05	0.13
Yb	0.69	0.46	1.11	0.38	1.08
Lu	0.11	0.07	0.16	0.05	0.14

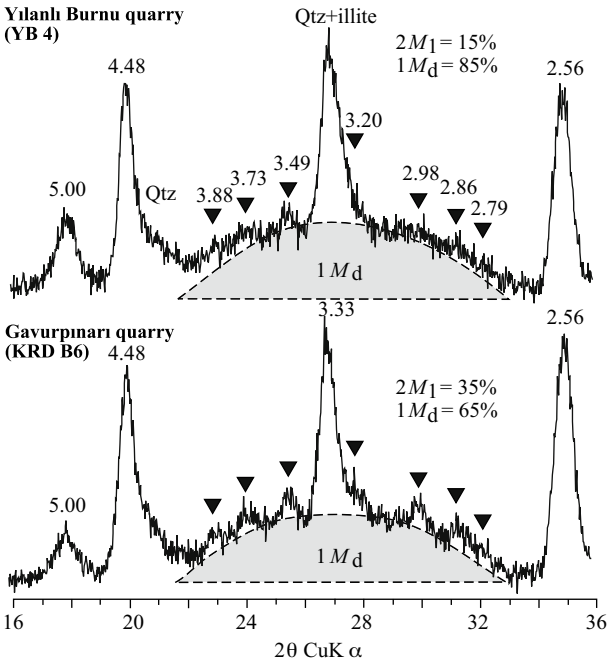

Figure 11. Unoriented powder diffraction patterns of the illite polytypes from Yılanlı Burnu (YB-4) and Gavurpınarı (KRD-B6) quarries.

6.4. Correlation with coeval occurrences and evaluation of the source area

A detailed correlation of the NW Anatolian K-bentonite levels with the globally recognized tephra chronological unit is hampered by the exact dating of the Turkish material. The currently available preliminary paleontological findings allow dating the tephra-formation in the Gavurpınarı area to the late Frasnian.

The closest locality known with Late Devonian tephra occurrences is in the southern Urals (Mizens, 2004; Vehrmarn et al., 2010). In the East Magnitogorsk zone in the central Urals, the late Frasnian is represented by porphyritic pyroxene and pyroxene-plagioclase basalt, and less often by andesite-basalt, trachybasalt, trachyandesite-basalt, associated lava breccias, tuff, tuffite, tephroid, tuffaceous conglomerate, and tuffaceous sandstone, occasionally with layers of rhyodacite tuff, siliceous rocks, and limestone. The thickness of the unit is 150–800 m. In the trachybasalt, anomalously high contents of Rb, K, Sr, Ba, Th, and light REEs, as well as raised contents of Nb, Ta, P, Hf, Zr Eu, Ti, and heavy REEs, were measured. Similar occurrences are reported from Siberia, Kazakhstan, and S China, ascribed to the closure of a number of small oceanic basins during the Altaid tectonic collage (e.g. Şengör and Natal'in, 1996).

Another candidate for the source of the NW Anatolian K-bentonites is the rift-related alkali basalts within the Donbas Basin on the eastern margin of the East European Craton. Radiometric age data indicate that the major stage of this volcanic activity was Late Devonian (380–355 Ma) in age (Alexandre et al., 2004). The geochemical composition and the age of this magmatic activity also correlate with the studied K-bentonites.

6.5. Concluding remarks

The analytical results have demonstrated that illitic clay beds, K-bentonites, intercalated with the limestones and dolomitic limestones of the Late Devonian Yılanlı formation in the Zonguldak-Bartın area were derived

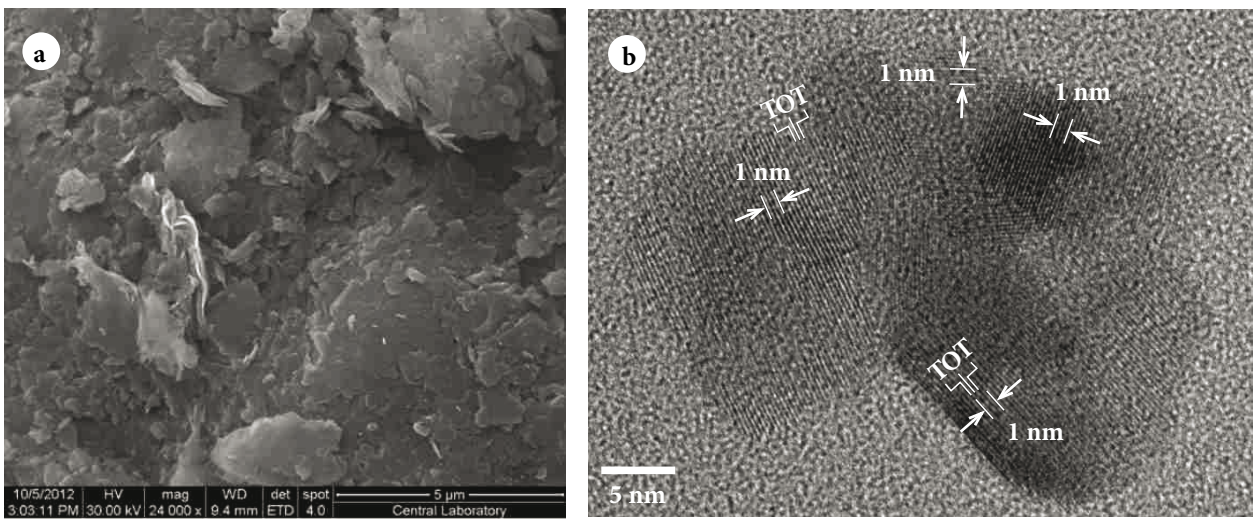

Figure 12. (a) SEM photomicrograph displays compacted, platy, and juxtaposed structure of illites in OC1-B3 sample from Gavurpınarı quarry. **(b)** HR-TEM microphotograph shows regular stacking sequence of illites (10 Å) in sample YBA-19A from Yılanlı Burnu quarry.

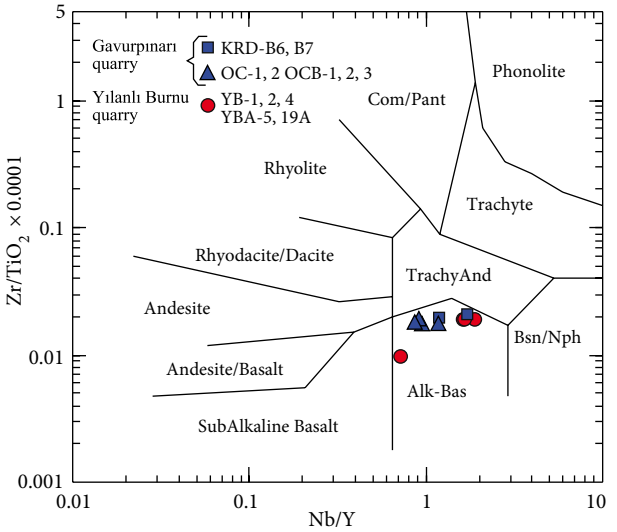

Figure 13. Original ash compositions of K-bentonites based on Zr/TiO_2-Nb/Y diagram of Floyd and Winchester (1978).

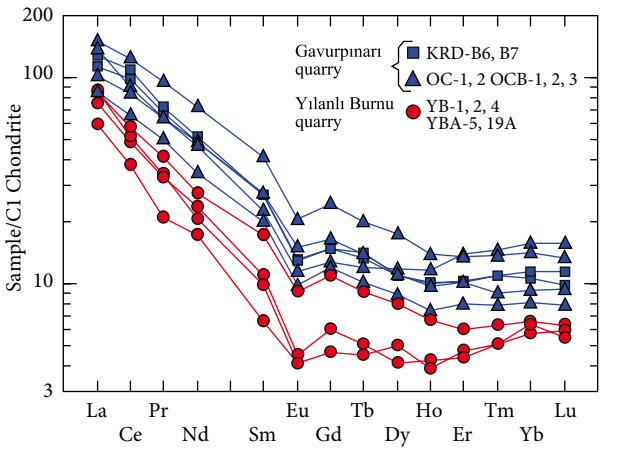

Figure 15. The chondrite-normalized REE diagram of K-bentonites.

from tephras deposited in a shallow marine environment by chemical modification and progressive illitization of smectite during the course until late diagenesis. These K-bentonites include volcanogenic nonclay minerals, zircon, biotite, feldspar, and quartz as another indicator of their volcanic origin.

The illite is the dominant clay mineral in the K-bentonites. Based on crystallo-chemical analyses, the degree of diagenesis has been determined as late diagenesis, which also resulted in regular stacking sequences (R > 3) for illite crystals because of illitization under high diagenetic conditions.

The studied K-bentonites were derived from a parent rock (tephra) with alkali-basaltic composition based on trace element discrimination. Their REE compositions point out that the parent tephras had a mantle source. The location of a volcanic source of K-bentonites observed in the Zonguldak-Bartın area might be in the northern part of the southern Urals, Siberia, or the Donbas Basin in the Scythian Platform and in East Europe, areas affected by Late Devonian volcanism having similar geochemical characteristics.

This study indicates the importance of K-bentonites from the western Black Sea region in terms of providing significant data about thermal maturation and subsidence history of the Zonguldak basin and their potential for long-distance stratigraphic correlations of Late Devonian strata.

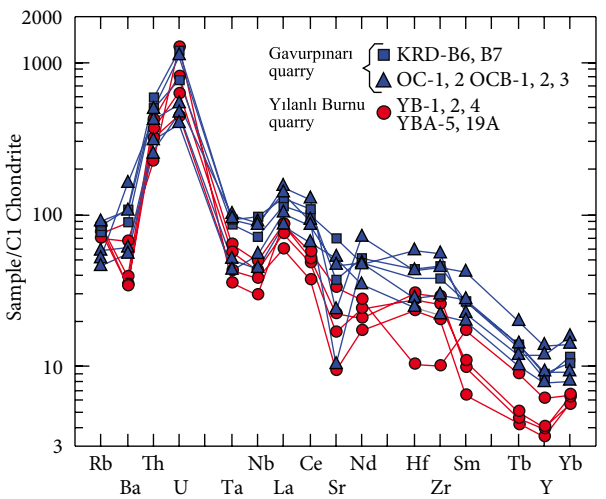

Figure 14. The chondrite-normalized trace element diagram of K-bentonites (normalization data from Sun and McDonough, 1989).

Acknowledgments

This study was supported by TÜBİTAK (Scientific Research Project Grant No. 110Y272). The authors thank Dr Warren D Huff (University of Cincinnati, USA) for valuable contributions during the preliminary field studies at the Gavurpinari limestone quarry, Dr Paul Schroeder (University of Georgia, USA) for grain size extractions and X-ray diffraction analysis, and the METU Central Laboratory for analytical support. The authors also thank Dr Işık Ece (İstanbul Technical University, Turkey) and an anonymous reviewer for their constructive comments.

References

Akbaş B, Altun IE, Aksay A (2002). 1/100.000 Ölçekli Türkiye Jeoloji Haritaları. Zonguldak-E28 Paftası. Ankara, Turkey: MTA Jeoloji Etütleri Dairesi (in Turkish).

Alexandre P, Chalot-Prat F, Saintot A, Wijbrans J, Stephenson R, Wilson M, Kitchka A, Stovba, S (2004). The $^{40}Ar/^{39}Ar$ dating of magmatic activity in the Donbas Fold Belt and the Scythian Platform (Eastern European Craton). Tectonics 23: 1–15.

Alişan C, Derman AS (1995). The first palynological age, sedimentological and stratigraphic data for the Çakraz Group (Triassic), western Black Sea. In: Erler A, editor. Geology of the Black Sea Region: Proceedings of the International Symposium on the Geology of Black Sea Region. Ankara, Turkey: General Directorate of Mineral Research and Exploration, pp. 93–98.

Allen VT (1932). Ordovician altered volcanic material in Iowa, Wisconsin, and Missouri. J Geol 40: 259–269.

Altaner SP, Ylagan RF (1997). Comparison of models of mixed-layer illite/smectite and reaction mechanism of smectite illitization. Clay Clay Miner 45: 517–533.

Aydın M, Serdar HS, Şahintürk O, Yazman M, Çokuğraş R, Demir O, Özçelik Y (1987). Çamdağ (Sakarya) - Sünnicedağ (Bolu) yöresinin jeolojisi. Bull Geol Soc Turkey 30/1: 1–4 (in Turkish).

Bailey SW (1988). X-ray diffraction identification of the polytypes of mica, serpentine, and chlorite. Clay Clay Min 36: 193–213.

Bethke CM, Vergo N, Altaner SP (1986). Pathways of smectite illitization. Clay Clay Miner 34: 125–135.

Bozkaya Ö, Yalçın H, Göncüoğlu MC (2012). Mineralogic evidences of a mid-Paleozoic tectono-thermal event in the Zonguldak terrane, NW Turkey: implications for the dynamics of some Gondwana-derived terranes during the closure of the Rheic Ocean. Can J Earth Sci 49: 559–575.

Bozkaya Ö, Yalçın H, Kozlu H (2011). Clay mineralogy of the Paleozoic-Lower Mesozoic sedimentary sequence from the northern part of the Arabian Platform, Hazro (Diyarbakır), Southeast Anatolia. Geol Carpath 62: 489–500.

Calarge L, Meunier A, Lanson B, Formoso M (2006). Chemical signature of two Permian volcanic ash deposits within a bentonite bed from Melo, Uruguay. Anais da Academica Brasileira de Ciencias 78: 525–541.

Chalot-Prat F, Tikhomirov P, Saintot A (2007). Late Devonian and Triassic basalts from the southern continental margin of the East European Platform, tracer of a single heterogeneous lithospheric mantle source. J Earth Syst Sci 116: 469–495.

Christidis GE (1998). Comparative study of the mobility of major and trace elements during alteration of an andesite and a rhyolite to bentonite in Island of Milos and Kimolos, Aegean, Greece, Clay Clay Miner 46: 379–399.

Dean WT, Martin F, Monod O, Demir O, Richards RB, Bultynck P, Bozdoğan N (1997). Lower Paleozoic stratigraphy, Karadere-Zirze area, Central Pontides, N Turkey. In: Göncüoğlu MC, Derman AS, editors. Early Paleozoic Evolution in NW Gondwana. Ankara, Turkey: Turkish Association of Petroleum Geologists Special Publication 3, pp. 32–38.

Derman AS (1997). Sedimentary characteristics of Early Paleozoic rocks in the western Black Sea region, Turkey. In: Göncüoğlu MC, Derman AS, editors. Early Paleozoic Evolution in NW Gondwana. Ankara, Turkey: Turkish Association of Petroleum Geologists Special Publication 3, pp. 24–31.

Dil N (1976). Assemblages caracteristiques de foraminiferes du Devonien superieur et du Dinantien de Turquie (Bassin Carbonifere de Zonguldak). Annales de la Societe Geologique de Belgique 99: 373–400 (in French).

Eberl DD, Velde B (1989). Beyond the Kübler index. Clay Miner 24: 571–577.

Floyd PA, Winchester JA (1978). Identification and discrimination of altered and metamorphosed volcanic rocks using immobile elements. Chem Geol 21: 291–306.

Fortey NJ, Merriman RJ, Huff WD (1996). Silurian and Late-Ordovician K-bentonites as a record of late Caledonian volcanism in the British Isles. T RSE Earth 86: 167–180.

Frey M (1987). Very low-grade metamorphism of clastic sedimentary rocks. In: Frey M, editor. Low Temperature Metamorphism. Glasgow, UK: Blackie, pp. 9–58.

Gedik İ, Pehlivan S, Duru M, Timur E (2005). 1:50.000 Scaled Geological Maps and Explanations: Sheets Bursa G22a and Istanbul F22d. Ankara, Turkey: General Directorate of Mineral Research Exploration.

Göncüoğlu MC, Dirik K, Kozlu H (1997). General characteristics of pre-Alpine and Alpine terranes in Turkey: explanatory notes to the terrane map of Turkey. Annal Géologique Pays Héllenique 37: 515–536.

Göncüoğlu, MC, Kozlu H (2000). Early Paleozoic evolution of the NW Gondwanaland: data from southern Turkey and surrounding regions. Gondwana Res 3: 315–324.

Göncüoğlu MC, Kozur HW (1998). Facial development and thermal alteration of Silurian rocks in Turkey. In: Gutierrez-Marco JC, Rabano I, editors.. Proceedings of the 1998 Silurian Field-Meeting. Madrid, Spain: Temas Geologico-Mineros ITGE 23, pp. 87–90.

Göncüoğlu MC, Kozur HW (1999). Remarks on the pre-Variscan development in Turkey. In: Linnemann U, Heuse T, Fatka O, Kraft P, Brocke R, Erdtmann BT, editors. Prevariscan Terrane Analyses of Gondwanean Europa. Dreseden, Germany: Schriften des Staatlichen Museums, Mineralogie, Geologie, pp. 137–138.

Göncüoğlu MC, Okuyucu C, Dimitrova T (2011). Late Permian (Tatarian) deposits in NW Anatolia: palaeogeographical implications. Geoecomarina 17: 79–82.

Göncüoğlu MC, Sachanski V, Gutiérrez-Marco JC, Okuyucu C (2014). Ordovician graptolites from the basal part of the Palaeozoic transgressive sequence in the Karadere area, Zonguldak Terrane, NW Turkey. Estonian J Earth Sci 63: 227–232.

Göncüoğlu MC, Saydam DG, Gedik İ, Okuyucu C, Özgül N, Timur E, Yanev S, Boncheva İ, Lakova İ, Sachanski V et al (2004). Correlation of the Paleozoic Units in Bulgaria and Turkey. Ankara, Turkey: MTA-BAS-TÜBİTAK 2004–16B4 Project Report.

Grathoff GH, Moore DM (1996). Illite polytype quantification using Wildfire© calculated X-ray diffraction patterns. Clay Clay Miner 44: 835–842.

Guggenheim S, Bain DC, Bergaya F, Brigatti MF, Drits V, Eberl DD, Formoso M, Galan E, Merriman RJ, Peacor DR et al (2002). Report of the Association Internationale pour L'etude des Argiles (AIPEA) Nomenclature Committee for 2001: order, disorder, and crystallinity in phyllosilicates and the use of the "crystallinity" index. Clay Clay Miner 50: 406–409.

Harries PJ (2009). Epeiric seas: a continental extension of shelf biotas. In: Cilek V, Smith RH, editors. Earth System: History and Natural Variability, Vol. IV. Oxford, UK: EOLSS Publishers, pp. 138–155.

Histon K, Klein P, Schonlaub HP, Huff WD (2007). Lower Palaeozoic K-bentonites from the Carnic Alps, Austria. Austrian J Earth Sci 100: 26–42.

Hoffman J, Hower J (1979). Clay mineral assemblages as low grade metamorphic geothermometers: application to the thrust-faulted disturbed belt of Montana, U.S.A. In: Scholle PA, Schluger R, editors. Aspects of Diagenesis. Tulsa, OK, USA: SEPM Special Publication 26, pp. 55–80.

Huff WD, Bergstrom SM, Kolata DR (1992). Gigantic Ordovician volcanic ash fall in North America and Europe: biological, tectonomagmatic and event-stratigraphic significance. Geology 20: 875–878.

Huff WD, Türkmenoğlu AG (1981). Chemical characteristics and origin of Ordovician K-bentonites along the Cincinnati Arch. Clay Clay Miner 29: 113–123.

Hunziker JC, Frey M, Clauer N, Dallmeyer RD, Frıedrichsen A, Flehmig W, Hochstrasser K, Roggwiler P, Schwander H (1986). The evolution of illite to muscovite: mineralogical and isotopic data from the Glarus Alps, Switzerland. Contrib Mineral Petr 92: 157–180.

Inoue A, Watanabe T, Kohyama A, Brusewitz AM (1990). Characterization of illitization of smectite in bentonite beds at Kinnekulle, Sweden. Clay Clay Miner 38: 241–249.

Kabanov PB, Betekhtin AN, Chikina NN, Fedorcov VV, Devyatka NP, Konstantinova MA, Khorosheva ON (2010). Automicrites, buildups, and reservoir shaping in Late Devonian basins of the East European Craton. In: GeoConvention 2010, Calgary, AB, Canada, 2010, p. 1–4.

Kalvoda J (2001). Upper Devonian-Upper Carboniferous foraminiferal paleobiogeography and Perigondwana terranes at the Baltica-Gondwana interface. Geol Carpath 52: 205–215.

Kay GM (1944a). Middle Ordovician of central Pennsylvania; Part 1, Chazyan and earlier Mohawkian (Black River) formations. J Geol 52: l–23.

Kay GM (1944b). Middle Ordovician of central Pennsylvania; Part 2, Later Mohawkian (Trenton) formations. J Geol 52: 97–116.

Keller WD, Reynolds RC, Inoue A (1986). Morphology of clay minerals in the smectite-to-illite conversion series by scanning electron microscopy. Clay Clay Miner 34: 187–197.

Kerey IE (1984). Facies and tectonic setting of the upper Carboniferous rocks of NW Turkey. In: Robertson AHF, Dixon J, editors. The Geological Evolution of the Eastern Mediterranean. Oxford, UK: Blackwell Scientific, pp. 123–128.

Kisch HJ (1991). Illite crystallinity: recommendations on sample preparation X-ray diffraction settings and inter-laboratory samples. J Metamorph Geol 9: 665–670.

Kolata DR, Huff WD, Bergstrom (1996). Ordovician K-bentonites of eastern North America. Geol Soc Am Spec Paper 313: 1–84.

Krumm S (1996). WINFIT 1.2: Version of November 1996 (The Erlangen Geological and Mineralogical Software Collection) of WINFIT 1.0: a public domain program for interactive profile analysis under WINDOWS. Acta Universitatis Carolinae Geologica 38: 253–261.

Kübler B (1968). Evaluation quantitative du metamorphisme par la cristallinite de l'illite. Bull Centre Rech Pau-SNPA 2: 385–397 (in French).

Lanson B, Velde B, Meunier A (1998). Late stage diagenesis of illitic clay minerals as seen by decomposition of X-ray diffraction patterns: contrasted behaviors of sedimentary basins with different burial histories. Clay Clay Miner 46: 69–78.

Lindgreen H, Hansen PL (1991). Ordering of illite-smectite in Upper Jurassic claystones from the North Sea. Clay Miner 26: 105–125.

Merriman RJ, Frey M (1999). Patterns of very low-grade metamorphism in metapelitic rocks. In: Frey M, Robinson D, editors. Low Grade Metamorphism. Oxford, UK: Blackwell, pp. 61–107.

Merriman RJ, Peacor DR (1999). Very low-grade metapelites: mineralogy, microfabrics and measuring reaction progress. In: Frey M, Robinson D, editors. Low Grade Metamorphism. Oxford, UK: Blackwell, pp. 10–60.

Merriman RJ, Roberts B (1990). Metabentonites in the Moffat Shale Group, Southern Uplands of Scotland: geochemical evidence of ensialic marginal basin volcanism. Geol Mag 127: 259–271.

Mizens GA (2004). Devonian palaeogeography of the Southern Urals. Geol Quart 48: 205–216.

Moore DM, Reynolds RC Jr (1997). X-Ray Diffraction and the Identification and Analysis of Clay Minerals. 2nd ed. Oxford, UK: Oxford University Press.

Nadeau PH, Wilson MJ, McHardy WJ, Tait JM (1985). The conversion of smectite to illite during diagenesis: evidence from some illitic clays from bentonites and sandstones. Mineral Mag 49: 393-400.

Nelson WA (1921). Notes on a volcanic ash bed in the Ordovician of Middle Tennessee. Tennessee Geological Survey Bulletin 25: 46–48.

Nelson WA (1922). Volcanic ash bed in the Ordovician of Tennessee. Geol Soc Am Bull 33: 605–616.

Nzegge OM, Satır MA, Siebel WA, Taubald HA (2006). Geochemical and isotopic constraints on the genesis of the Late Palaeozoic Deliktaş and Sivrikaya granites from the Kastamonu Granitoid Belt (Central Pontides, Turkey). Neues Jb Miner Abh 183: 27–40.

Okay N, Zack T, Okay AI (2010). A missing provenance: sandstone petrography and detrital zircon-rutile geochronology of the Carboniferous flysch of the Istanbul zone. In: Tectonic Crossroads: Evolving Orogens of Eurasia-Africa-Arabia. Ankara, Turkey: Geological Society of America, p. 67.

Racki G, Sobon-Podgorska J (1993). Givetian and Frasnian calcareous microbiotas of the Holy Cross Mountains. Acta Palaent Polonica 37: 255–289.

Rosenkrans RR (1934). Correlation studies of the central and south-central Pennsylvania bentonite occurrences. Am J Sci 17: 113–134.

Sabirov AA (2004). Pre-Visean foraminifers from Central Asia and Kazakhstan. Paleontol J 38: 238–246.

Sachanski V, Göncüoğlu MC, Gedik I (2010). Late Telychian (early Silurian) graptolitic shales and the maximum Silurian highstand in the NW Anatolian Palaeozoic terranes. Palaeogeogr Palaeoecl 291: 419–428.

Şengör AMC, Natal'in BA (1996). Paleotectonics of Asia: fragment of a synthesis. In: Yin A, Harrison TM, editors. The Tectonic Evolution of Asia. Cambridge, UK: Cambridge University Press, pp. 486–640.

Środoń J (1984). X-ray powder diffraction identification of illitic materials. Clay Clay Miner 32: 337–349.

Sun SS, McDonough WF (1989). Chemical and isotopic systematics of oceanic basalts: implications for mantle composition and process. In: Saunders AD, Norry MJ, editors. Magmatism in Ocean Basins. London, UK: Geological Society of London Special Publication 42, pp. 313–345.

Türkmenoğlu AG (2001). A Paleozoic K-bentonite occurrence in Turkey. In: Mid-European Clay Conference'01, Stara Leusa, Slovakia, Book of Abstracts, p. 108.

Türkmenoğlu AG, Göncüoğlu MC, Bayraktaroğlu Ş (2009). Early Carboniferous K-bentonite formation around Bartın: geological implications. In: 2nd International Symposium on the Geology of the Black Sea Region, İstanbul, Turkey, p. 209.

Vachard D (1991). Parathuramminides et Moravamminides (Microproblematica) de l'emsien superieur de la formation Moniello (Cordilleres Cantabriques, Espagne). Revue de Paléobiologie 10: 255–299 (in French).

Vachard D (1994). Foraminiferes et Moravamminides du domaine Ligerien (Massif Armoricain, France). Palaeontographica Abt A 231: 1–92 (in French).

Warr LN, Rice AHN (1994). Interlaboratory standardisation and calibration of clay mineral crystallinity and crystallite size data. J Metamorph Geol 12: 141–152.

Weaver CE (1953). Mineralogy and petrology of some Ordovician K-bentonites and related limestones. Geol Soc Am Bull 64: 921–944.

Weaver CE (1961). Clay minerals of the Ouachita structural belt and adjacent foreland. In: Flawn PT, Goldstein A Jr, King PB, Weaver CE, editors. The Ouachita Belt. Austin, TX, USA: University of Texas Geology Publication 6120, pp. 147–162.

Wehrmann A, Yılmaz İ, Wilde V, Yalçın MN, Schindler E (2010). The Devonian coastline of northern Gondwana: sedimentary signatures of depositional environments at the land-sea transition (Taurides, Turkey). In: 7th International Symposium on Eastern Mediterranean Geology, Çukurova University, Adana, Turkey, p. 55.

Winchester JA, Floyd PA (1977). Geochemical discrimination of different magma series and their differentiation products using immobile elements. Chem Geol 20: 325–344.

Yalçın MN, Yılmaz İ (2010). Devonian in Turkey – a review. Geol Carpath 61: 235–253.

Yanev S, Göncüoğlu MC, Gedik I, Lakova I, Boncheva I, Sachanski V, Okuyucu C, Ozgul N, Timur E, Maliakov Y et al. (2006). Stratigraphy, correlations and palaeogeography of Palaeozoic terranes of Bulgaria and NW Turkey: a review of recent data. In: Robertson AHF, Mountrakis D, editors. Tectonic Development of the Eastern Mediterranean Region. London, UK: Geological Society of London Special Publication 260, pp. 51–67.